Adsorption 4, 299–311 (1998)

Full Analysis of Internal Adsorbate Redistribution in Regenerative Adsorption Cycles

M. PONS
C.N.R.S.-L.I.M.S.I., B.P. 133, F-91403 ORSAY CEDEX, France

Abstract. Adsorption cycles with heat regeneration are a promising CFC-free alternative to compression cycles, for refrigeration or heat pumping purposes. However, the process is complex and therefore requires efficient analysis tools to understand correctly. These tools are now developed and used here for studying the phenomenon of internal adsorbate redistribution. This phenomenon takes place during the periods when the adsorber is pressurised, or depressurised, under globally isosteric conditions. It can be easily thought that internal adsorbate redistribution reduces the cycle performance. In order to avoid this reduction, the adsorbate redistribution can be reduced by implementing separate vapour compartments inside the adsorbers, which also requires the installation of additive check valves between the adsorber, condenser and evaporator.

The present study shows that, in fact, this phenomenon does not affect performance. In addition, thanks to the different analysis tools, a physical explanation of this result, based on first and second laws of thermodynamics is developed. This result is then valid for any heat regenerative cycle using an adsorption pair.

Keywords: entropy, heat pump, refrigeration, heat regeneration

Introduction

Microporous adsorbents such as zeolites or active carbons are widely used in separation or purification processes and also as catalysts for chemical reactions. Refrigeration or heat pumping only represents a minor part of the market of adsorbents; however, adsorptive refrigeration systems are likely to offer a high performance CFC-free alternative to compression cycles. Indeed, by alternating periods of heating and cooling, adsorbents can be used as 'thermal compressors' and can therefore power refrigeration cycles. As a matter of fact, air conditioners using open cycle desiccant cooling, mainly with silicagels, are already on the market and academic studies of such systems are still developing (Collier and Cohen, 1991; Kuma et al., 1995). Adsorption closed cycles with zeolites appeared to be quite efficient for solar refrigeration (Grenier et al., 1988) but their performance must be significantly enhanced when competition with compression cycles is aimed. Thermodynamic efficiency of adsorption cycles is increased when part of the energy required for heating the adsorber is internally recovered from heat rejected by the system itself (Meunier, 1993). Among different possibilities, the process termed as 'temperature front', 'thermal wave' or 'heat regeneration' is very promising. The principle is to generate in the adsorber a significant and unstationary temperature gradient along the flow of the heat transfer fluid (HTF). Due to this 'thermal wave', the adsorber is used like a 'heat regenerative' thermal storage. This technique permits recovering 75–80% of the energy stored in an adsorber/reactor (Shelton et al., 1990; Härkönen and Aittomaki, 1991). Indeed, more and more studies are dedicated to such systems (Hajji and Worek, 1991; Jones, 1993; Ludwig, 1995; Zheng et al., 1995a, 1995b; Critoph, 1996a; Miles and Shelton, 1996; Pons et al., 1996; Pons and Szarzynski, 1996).

Heat regenerative cycles can also be developed with other solid-gas systems. In the field of chemical reaction systems, they are termed as 'multisalt' (Istria et al., 1995, 1996). In the field of hydride systems, they are termed as 'multihydride' (Willers et al., 1996). It must be noticed that these two latter solid-gas systems are

ruled by a monovariant equilibrium. As a consequence, for the chemical reaction (or hydriding) reaction to process simultaneously at a prescribed pressure but at different temperatures, several salts (or hydriding alloys) must be implemented in the reactor. Istria et al. (1996) have shown that the efficiency of the heat regenerative cycles increases with the number of individual salts implemented in the reactor.

As adsorptive systems are ruled by a divariant equilibrium, adsorption or desorption proceeds naturally at a prescribed pressure and over a continuous range of temperature. In other words, adsorbents naturally offer the equivalent of an infinite number of salts (or hydrides) in the reactor. The divariant equilibrium is then a large advantage in favour of the adsorption systems.

However, Guilleminot (1987) described a side-effect that takes place in an adsorbent bed undergoing pressure change under globally isosteric conditions: the internal adsorbate redistribution. This phenomenon, which is specific to adsorption systems (it does not occur in the above-mentioned monovariant systems), leads to a problem which is altogether academic and practical. Indeed, it was first thought that this phenomenon would reduce the performance of the heat regenerative cycles. It would then have been necessary to separate the future regenerative adsorbers into compartments that cannot exchange adsorptive vapour and to equip each of them with two check valves, one for condensation, the other one for evaporation. The study of a particular case has shown that this phenomenon actually does not change the cycle performance (Pons and Szarzynski, 1996). Making the analysis more general will permit demonstrating that it is the case for any adsorption system. The present article develops a full (i.e., first and second laws) analysis of this phenomenon.

In the first section, the adsorption cycles with heat regeneration are described. Then the phenomenon of internal adsorbate redistribution, and a powerful tool for second law analysis of sorption cycles (the diagram Entropic Mean Temperature versus Entropy) are presented. The second section presents the implementation of two compartments in the adsorber and the different changes induced by reducing the internal adsorbate redistribution. All the results are yielded by a model that is presented in Appendix, where the modelling of the adsorption source term is emphasised. For sake of simplicity, all the equations and graphs presented are established for the case of a cylindrical adsorber where the heat transfer fluid flows in the axial direction and where the radial temperature gradients in the adsorbent bed are not significant. In the third section, the first and second laws analyses of the internal adsorbate redistribution are developed, which leads to the conclusion.

Adsorber with One Vapour Compartment

Principle of Adsorption Cycles with Heat Regeneration

It is known for long that adsorption systems can be used for refrigeration or heat pumping cycles (Miller, 1929). These cycles consist of two periods. In the first period, the adsorbent is heated at high pressure thereby inducing desorption of refrigerant vapour that can be liquefied in a condenser. In the second period, the adsorbent is cooled at low pressure, which makes it adsorb the vapour produced by the evaporation of the liquid refrigerant. The cooling effect is due to this evaporation. In order to enhance performance of an adsorption unit, it can comprise two adsorbers that are operated out of phase and that are also used as thermal storage for the internal heat recovery. Figure 1 presents the principle of adsorption cycles with non-uniform temperatures, in which the adsorbers are used as heat regenerative thermal storages. The two adsorbers, the heating system and the cooling system are installed in series in a heat transfer fluid (HTF) loop, where the HTF is circulated by a reversible pump. When the HTF undergoes large

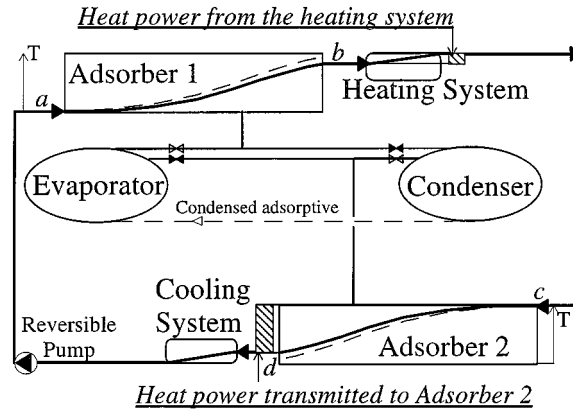

Figure 1. Principle of the adsorption cycle with thermal regeneration. Thank to the energy released by Adsorber 1, only a limited energy is required from the heat source in order to transmit a large energy to the Adsorber 2. The inlet fluid temperatures (points *a* and *c*) are resp. T_{CS} and T_{HS}. The outlet fluid temperatures (points *b* and *d*) vary in time.

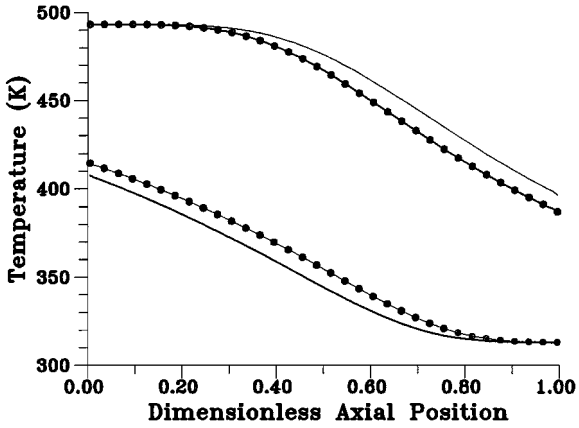

Figure 2. Temperature profiles at the end of each period of cycle 1 (See Table 1) in periodical operation: HTF (solid lines) and adsorbent: (•).

temperature difference between the inlet and outlet of each adsorber, then the heat power to be supplied by the heating system is much less than that transmitted to the adsorber being heating up. This reduction of the energy demand from the heat source obviously makes the cycle more efficient. In order to maintain the advantage of the situation described in Fig. 1, the flow direction must be changed at the appropriate moment (Zheng et al., 1995b; Pons et al., 1996; Pons and Szarzynski, 1996; Pons, 1996). These studies also show that the temperature profiles in each component of the adsorber (the HTF, metal and adsorbent) at the moment of flow reversal are absolutely non-uniform. An example is given in Fig. 2. The temperature profiles in the adsorbent are important because they determine the amount of refrigerant that is cycled during a half-cycle, Δm:

$$\Delta m = \int_0^L A_s \cdot \rho_s \cdot \left[\varepsilon_{(T_s(z,tc/2),P_e)} - \varepsilon_{(T_s(z,0),P_c)}\right] \cdot dz \tag{1}$$

Equation (1) is calculated during the cooling half-cycle ($\Delta m > 0$). Δm directly determines the heat extraction during the half-cycle, Q_e:

$$Q_e = \Delta m \cdot [L_{\text{ev}} - C_{pL} \cdot (T_c - T_e)] \tag{2}$$

The studies discussed above have also shown that the temperature profiles depend on the operating conditions, especially on the cycle period.

It must be remarked that the expression 'heat regeneration' does not mean herein that the adsorbent is 'regenerated' with thermal energy, because it is always so in any type of adsorptive refrigeration cycle. This expression means that the technique of 'heat regenerative thermal storage' is used in order to recover energy within the process. It must also be remarked that the vapour phase in the unit only contains pure refrigerant vapour. In the refrigeration cycle, the adsorbent temperature is, by principle, always above the saturation temperature that corresponds to the vapour pressure in the bed at the considered moment. As a consequence, although the cycle with heat regeneration presented in Fig. 1 can evoke the TSA process, the refrigerant vapour that is in the bed is always super-heated and it cannot condense within the adsorbent column. In addition, in the present case, the heat transfer media is not the refrigerant, which makes another difference from the TSA process.

Modelling

The temperature profiles presented in Fig. 2 are calculated by a model. Several modellings of the adsorber operated with a thermal wave have been developed: two- dimensional models (Hajji and Worek, 1991; Miles and Shelton, 1991; Sun et al., 1995; Zheng et al., 1995a, 1995b), 3-temperature models (Sun et al., 1997), and 2-temperature models (Fueller et al., 1994). The 3-temperature model developed by Sun et al. (1997) is used in the following. It relies on the following assumptions: the adsorption pair is always in equilibrium (vapour and solid are at the same temperature, adsorption kinetics is very fast) and the vapour pressure is uniform in the bed; the temperatures of heat source, heat sink, condenser and evaporator are fixed and constant (ideal heat sources); axial thermal conduction in metal and adsorbent is negligible; the physical characteristics (ρ, λ, C_{p}, etc.) of the HTF, metal, adsorbent and refrigerant are constant; the sorption process is modelled with an exact heat source term (see Appendix). The modelled adsorber geometry is shown in Fig. 3. The adsorber consists of a group of sixteen 1.2-m long cells in parallel. Each cell consists of two coaxial cylinders. The inner one for the HTF (Dowtherm Q), the outer one for the adsorbent (1 kg of anhydrous pure zeolite NaX). The adsorbent is a very anisotropic composite (zeolite NaX + Expanded Natural Graphite) with very good heat transfer and mass transfer characteristics (resp. a thermal conductivity of 15 $\text{W} \cdot \text{m}^{-1} \cdot \text{K}^{-1}$ and a permeability of 10^{-9} m^2) in the radial direction but very poor ones in the axial direction, which corresponds to the model assumptions.

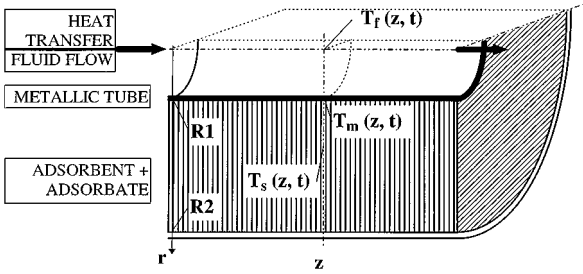

Figure 3. Schematic representation of the modelled geometry. The heat transfer fluid flows in the inner cylinder (R1 = 3 mm), the adsorbent bed lies in the outer cylinder (R2 = 7.5 mm). An external dead volume makes the vapour pressure constant all along the adsorber and provides a thermal insulation.

An external dead volume filled with refrigerant vapour makes the pressure uniform in the whole adsorber. As the refrigerant is water, the saturation pressure at the condensation temperature (40°C) is quite low (7400 Pa) and the vapour mass contained in this dead volume is negligible. The model is described in the Appendix. Once the heat source temperatures, adsorber characteristics, fluid flow rate and cycle period are fixed, the model is run until periodical operation is attained.

Breakthrough Curve and Pressure Variation

One adsorption cycle with heat regeneration, typical for airconditioning application, is first modelled. Its characteristics and performance are given in Table 1 (cycle 1). Figure 2 presents the temperature profiles in the adsorber at the end of the cooling and heating periods. Figure 4 is very useful for comprehensive understanding of the present problem. Figure 4(a) presents the "breakthrough curve", i.e., the time variation of the fluid temperature at the outlet of the adsorber

Table 1. Characteristics and performance of the cycles investigated.

Cycle	Figure	Cooling COP	Cooling power (W)
1	4 and 6	0.92	205
2	8 and 9	0.92	205
3	10	0.92	206
5	10	0.93	206

Characteristics: Adsorption pair: Zeolite NaX + Water; 1 kg anhydrous zeolite powder + graphite binder; Heat source temperatures: $T_{HS} = 220°C$; $T_{CS} = T_c = 40°C$; $T_e = 3°C$; Heat transfer surface = 0.33 m^2; HTF flow rate = 5.6 g · s^{-1}; Global number of transfer units between the adsorbent and HTF = 12.9; Cycle period = 700 s.

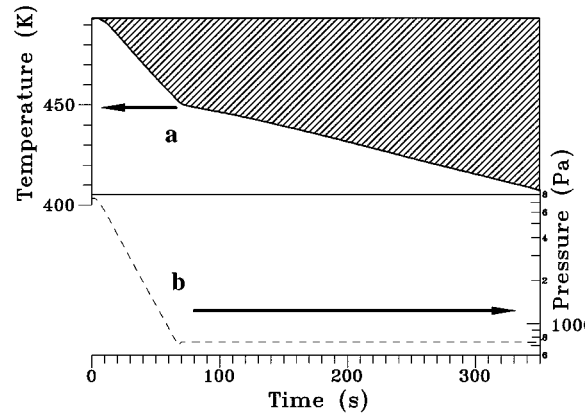

Figure 4. Breakthrough curve (a) and pressure evolution (b) during the cold period of cycle 1. The hatched region represents the energy supplied by the heat source.

during the cooling-adsorption-evaporation period. Indeed, as shown in Fig. 1, the heat power required from the heating system is proportional to the temperature difference between the heat source temperature and this outlet fluid temperature:

$$\dot{Q}_{HS} = \dot{m}_f \cdot C_{pf} \cdot \left(T_{HS} - T_f^{o,c}\right) \qquad (3)$$

As the product ($\dot{m}_f \cdot C_{pf}$) is almost constant, the total energy required from the heating system during a half-cycle is proportional to the hatched surface lying above the breakthrough curve in Fig. 4(a).

Figure 4(b) presents the parallel time variation of the vapour pressure in the adsorber. This curve exhibits two parts. In the first one (from 0 to 68 seconds), the vapour pressure decreases: this is the depressurisation period in globally isosteric conditions. In the second part, the pressure is constant and equals the vaporisation pressure: this is the evaporation- adsorption period. It can be observed in Fig. 4(a) that the breakthrough curve presents a remarkable knee at exactly the same moment: 68 seconds. In the first part (globally isosteric depressurisation), the outlet fluid temperature decays rapidly while the decay is significantly slower during the second part (adsorption at constant pressure). A significant reduction of the energy supplied by the heat source and therefore a significant enhancement for the cycle COP would result from a slower temperature decay during the globally isosteric subperiod. Internal adsorbate redistribution, which occurs during this subperiod, is likely to play a role in this rapid decay of the breakthrough curve. Therefore, it can be worth studying this phenomenon.

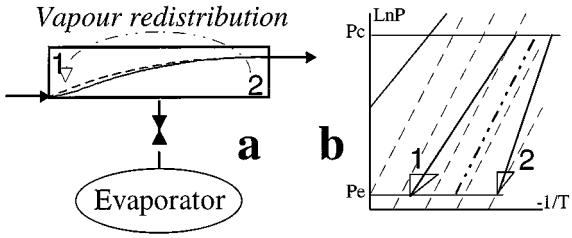

Figure 5. Description of the vapour redistribution in a closed adsorber during the cooling period: in a schematic adsorber (a) and in the Clapeyron diagram (b): the region with faster temperature decay (1) adsorbs vapour when the region with slower temperature decay (2) desorbs vapour.

Internal Adsorbate Redistribution

This phenomenon, that takes place in a closed adsorbent volume undergoing non-uniform temperature changes, was first described by Guilleminot et al. (1987) and has been since then mentioned by several authors (Miles et al., 1993; Zheng et al., 1995c; Critoph, 1996b). It concerns almost any adsorber being pressurised (or depressurised) in globally isosteric conditions, especially in the cycles with heat regeneration. This phenomenon is described here, with the help of Fig. 5, in the case of a cooling period under uniform pressure. However, everything is symmetrical in the heating case and a non-uniform pressure in the adsorbent bed reduces the redistribution of adsorbate but does not cancel it.

When the cold heat transfer fluid starts flowing into the adsorber, entering it on the cold side of the adsorber, the adsorbent located close to the fluid inlet (Region 1 in Fig. 5) undergoes a faster temperature decay than that located at the other end of the adsorber (Region 2). Meanwhile, because of the globally isosteric condition, the pressure 'follows' the variation of the average temperature in the adsorber. Because of the non-uniform temperature variations, the adsorbent located in Region 1 undergoes a temperature decay faster than this average temperature while the temperature decay in the adsorbent located in Region 2 is slower. As a consequence, the adsorbent located in Region 1 adsorbs vapour, while that located in Region 2 desorbs vapour: some adsorbate is redistributed inside the adsorbent bed (see Fig. 5(b)). This phenomenon has special consequences for the cycles with heat regeneration. Indeed, adsorption is exothermic. Due to the adsorbate redistribution, adsorption heat is released there where vapour is adsorbed (Region 1) and adsorption heat is consumed there where vapour is desorbed (Region 2). It results

Table 2. Summary of the internal adsorbate redistribution.

In the adsorbent close to the Heat Transfer Fluid...	inlet (1)	outlet (2)
temperature decays ...	faster	slower
than average, some vapour is ...	adsorbed	desorbed
adsorption heat is ...	released	consumed
temperature decay rate is ...	reduced	increased
Temperature front is less steep		
Outlet fluid temperature decays more rapidly		

Table 3. Values of the adsorbate concentration (in $g \cdot kg^{-1}$) at different moments of a cooling half-cycle and at different locations in the adsorber: inlet, outlet and two adjacent points in the middle of the adsorber. The points 'F, G, W and X' indicated correspond to the ones presented in Fig. 9. Case of a cycle with only one vapour compartment: the adsorber is closed from 0 to 68 seconds and connected to the evaporator from 68 to 350 seconds.

		Two adjacent points middle of adsorber		
Time (s)	Inlet of the HTF (Point G)	(Point W)	(Point X)	Outlet of the HTF (Point F)
0	225	91	88	58
47	273	89	86	44
68	274	89	87	39
350	279	200	197	83

that internal adsorbate redistribution reduces the temperature difference between the inlet and the outlet of the adsorber. In other words, it reduces the steepness of the temperature front. Moreover, it also makes the outlet fluid temperature decay faster during the subperiod of globally isosteric cooling. Table 2 summarises the description of the phenomenon. Table 3 shows the variations during the cooling half-cycle of the adsorbate concentration ε at different locations in the adsorbent bed: inlet of the HTF (i.e., Region 1), outlet of the HTF (i.e., Region 2) and two adjacent points in the middle of the adsorber. The internal adsorbate redistribution during the globally isosteric subperiod (0–68 s) clearly appears: ε 'at the inlet' (Region 1) increases ($+49$ $g \cdot kg^{-1}$) when ε 'at the outlet' (Region 2) decreases (-19 $g \cdot kg^{-1}$). Meanwhile, ε is practically unchanged (-2 $g \cdot kg^{-1}$) in the middle of the adsorber: only this centre part of the adsorber is almost isosteric. Let us now consider the next subperiod, the one with adsorption and evaporation: 68–350 s. First, ε 'at the inlet' is almost unchanged ($+5$ $g \cdot kg^{-1}$). Second, ε 'at the outlet' increases ($+44$ $g \cdot kg^{-1}$) more than its

decrease during the first subperiod. Third, the major part of the adsorption takes place in the middle of the adsorber ($+110\ \mathrm{g \cdot kg^{-1}}$). Table 3 shows that, because of the adsorbate redistribution, the 'adsorption history' is completely different in the different points of the adsorbent bed. The adsorbent located in Region 1 adsorbs very soon (before 47 s) almost all the refrigerant that it will finally adsorb. This refrigerant early adsorbed does not come from the evaporator but from the other side of the adsorber, the hot side. The adsorbent located around the middle of the adsorber is first almost isosteric and adsorbs later on a lot of vapour from the evaporator. The adsorbent in Region 2 first desorbs vapour toward the Region 1 and, later, adsorbs from the evaporator more vapour than firstly desorbed.

It can also be noticed from Table 3 that the internal adsorbate redistribution mainly occurs in the first part of the globally isosteric subperiod (before 47 s).

Description of the Adsorption Cycle with Heat Regeneration in the $\tilde{T} - \Delta S$ Diagram

The general definition of the entropic mean temperature $\tilde{T}$ is given in Appendix. The analysis of solid sorption cycles with the help of the concept of entropic mean temperature permits defining equivalent Carnot cycles (Neveu and Castaing-Lasvignottes, 1996; Meunier et al., 1997). This approach is very powerful for describing the efficiency of the different processes and the internal irreversibilities involved in the adsorption cycles. This analysis has also been developed for the adsorption cycles with heat regeneration (Pons, 1997). The "3-temperature" model mentioned above has been used for calculating the different heat exchanges in the cycle: first, between the HTF and the heating or cooling systems; second, between the refrigerant and condenser or evaporator; and between the HTF and the adsorber.

In the latter case, it must be remembered that temperature is basically not uniform in the adsorber. Therefore, $\tilde{T}$ is a function of the axial position z. Each heat exchange corresponds to an entropy change ΔS and a value of $\tilde{T}$. When only sensible heat is involved, ΔQ, ΔS and $\tilde{T}$ are easily calculated. The case of a portion of the adsorber where both sensible heat and sorption latent heat are involved is detailed in the Appendix.

Adsorption cycles with heat regeneration must be represented in the $\tilde{T} - \Delta S$ diagram by two cycles,

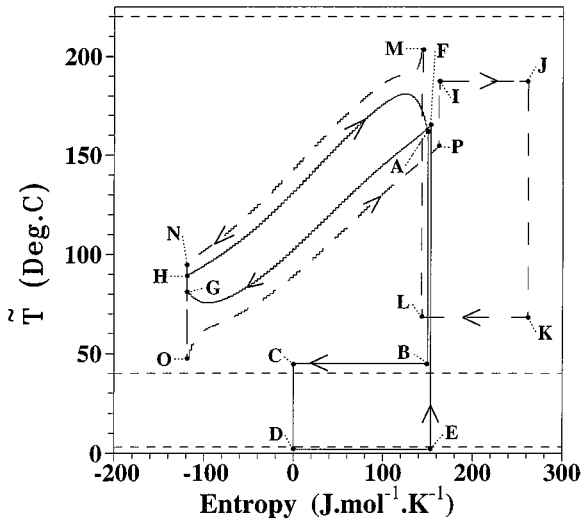

Figure 6. Representation of a typical adsorption cycle with thermal regeneration in the $\tilde{T} - \Delta S$ entropic diagram. The entropy changes are per mole of cycled adsorptive. Adsorption system: cycle ABCDEFGH in solid lines; HTF system: cycle IJKLMNOP in dashed lines. The temperatures of the heat sources/sinks are displayed (horizontal dashed lines). The presented cycle is the cycle 1 (see characteristics in Table 1).

see Fig. 6. The first one, ABCDEFGH, represents the adsorption system: condenser (branch BC), evaporator (branch DE), adsorber in cooling phase (FG) and adsorber in heating phase (HA). The second one, IJKLMNOP, represents the "HTF system", i.e., the different heat exchanges involving the HTF: heat source at high temperature (branch IJ), heat sink at intermediate temperature (KL), adsorber in the heating phase (MN) and adsorber in the cooling phase (OP). The non-uniformity of temperature in the adsorber can be seen on the branches FG, HA, MN and OP. Figure 6 is widely commented in (Pons, 1997), where a paradox is mentioned: the point A represents the location with maximal temperature in the adsorber, however $\tilde{T}$ is not maximal at this point but somewhere else on the branch HA. Similarly, the point G represents the location with minimal temperature in the adsorber but $\tilde{T}$ is minimal somewhere else on the branch FG. It will be seen in the following that this paradox is due to the internal adsorbate redistribution. Besides, as the branch FG represents the adsorber during the cooling half-cycle, the points G and F respectively correspond to the points 'at the HTF inlet' (Region 1) and 'at the HTF outlet' (Region 2) of Table 3.

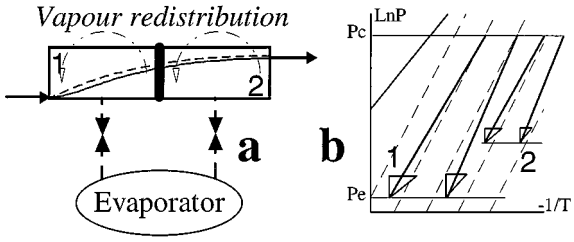

Figure 7. Description of the behaviour of an adsorber with two separate vapour compartments during the cooling period: in a schematic adsorber (a) and in the Clapeyron diagram (b). Pressure is lower in compartment (1) than in compartment (2): the former one is connected to the evaporator before the latter one.

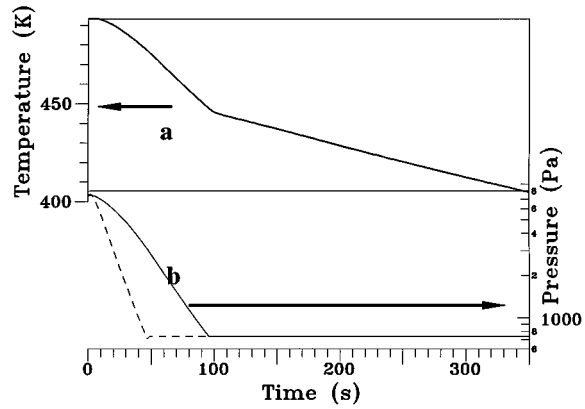

Figure 8. Breakthrough curve (a) and pressure evolution (b) during the cold period of cycle 2. The dashed line shows the pressure in compartment 1, the solid line that in compartment 2.

Adsorber with Two Vapour Compartments

Principle and Description of an Adsorber with Two Compartments

In order to partially prevent the internal redistribution of adsorbate, the adsorber can easily be separated into two equal parts, one on the 'cold side' of the adsorber, one on the 'warm side'. The adsorbent mass is equally divided between them. The HTF flows through these two halves in series, but vapour cannot flow from one compartment to the other one. Therefore, each compartment needs its own pair of valves for connection to the condenser and evaporator. The operation of an adsorber with two vapour compartments is described in Fig. 7. Now, vapour can be redistributed only within each compartment and vapour pressure can be different in each compartment, especially when one of them is closed.

After adaptation of the model (Szarzynski et al., 1997), the same cycle as that formerly presented is calculated for an adsorber with two vapour compartments (see Appendix). The characteristics and performance of the cycle are presented in Table 1 (cycle 2). It can be seen that the performance data for cycle 2 are the same as for cycle 1: same COP, same cooling power. The temperature profiles are not presented here because they differ from the ones presented in Fig. 2 by a fraction of Kelvin only. This latter fact means that the cycled mass of refrigerant is almost unchanged, and consequently so is the cooling load.

Figure 8 presents the breakthrough curve and the time variation of vapour pressure in each compartment during a cooling half-cycle. The vapour pressure decays more rapidly in compartment 1 than in compartment 2. It can also be seen that, in the very first part of the curve (0–47 s), the decay of the breakthrough curve is indeed much slower than that shown in Fig. 4(a). The analysis developed in Table 2 is then correct, at least for this first subperiod. However, the pressure in compartment 1 reaches the evaporation pressure before that in compartment 2 (respectively, 47 and 96 s). Compartment 1 is then connected to the evaporator first. As a consequence, the cooling period now consists of three parts. In the first one (0–47 s), both compartments are closed and cooled in globally isosteric conditions. In the second part (47–96 s), only the compartment 1 is open and adsorbs vapour from the evaporator, while the compartment 2 is still closed. In the third part (96–350 s), both compartments are open and adsorb vapour. It can be observed that the knee in the breakthrough curve in Fig. 8(a) is delayed up to when the second compartment eventually opens (96 s). However, the corresponding outlet fluid temperature is lower than that in Fig. 4(a) at the same moment: 445 K instead of 450 K. As a matter of fact, it results that the surface lying above the breakthrough curve is unchanged: both cycles require the same heat input from the heat source. Same cooling load, same heat input: these two cycles have exactly the same performance, as can be seen in Table 1.

Table 4 shows the same quantities as Table 3, but calculated for this cycle 2 at different moments: 0, 47, 96 and 350 s. The reduction of the adsorbate redistribution clearly appears: between 0 and 47 s, ε at the 'inlet' (point G) increases, but less than in cycle 1 ($+39$ g $\cdot$ kg^{-1} instead of $+48$ g $\cdot$ kg^{-1}). Simultaneously, ε at the 'outlet' (point F) decreases, but less than in cycle 1 (-7 g $\cdot$ kg^{-1} instead of -14 g $\cdot$ kg^{-1}). Let us now observe what happens in the adsorbent located on either

Table 4. Values of the adsorbate concentration (in $g \cdot kg^{-1}$) at different moments of a cooling half-cycle and at different locations in the adsorber: inlet, outlet and two adjacent points in the middle of the adsorber. The points 'F, G, W and X' indicated correspond to the ones presented in Fig. 9. Case of a cycle with two vapour compartments: from 0 to 47 seconds both compartments are closed, from 47 to 96 seconds only compartment 2 is closed and from 96 to 350 seconds the whole adsorber is connected to the evaporator.

Time (s)	Inlet of the HTF (Point G)	Two adjacent points middle of adsorber (Point W)	(Point X)	Outlet of the HTF (Point F)
0	223	94	92	58
47	262	85	108	51
68	273	102	116	41
350	279	199	196	87

side of the separation, i.e., at point W, which is in the middle of the adsorber but in compartment 1, and at point X, which is in the middle of the adsorber but in compartment 2. Table 4 shows that ε at point W decreases ($-9\ g \cdot kg^{-1}$) when ε at point X increases ($+16\ g \cdot kg^{-1}$). These points in the middle of the adsorber, that were almost isosteric in cycle 1, are now involved in the adsorbate redistribution. Table 4 also shows that, in the next subperiod (47–96 s), ε increases in compartment 1 (points G and W) while adsorbate redistribution still significantly proceeds in compartment 2 ($+8\ g \cdot kg^{-1}$ at point X and $-10\ g \cdot kg^{-1}$ at point F).

Representation in the $\tilde{T} - \Delta S$ Diagram

The $\tilde{T} - \Delta S$ cycle of the regenerative adsorption cycle with two vapour compartments is shown in Fig. 9. Comparing it to Fig. 6, it can first be noticed that none of the global entropy changes in the cycle is modified. Nevertheless, modifications can be observed on the branches FG, HA, MN and OP: these branches now exhibit two sections. Indeed, each section corresponds to one vapour compartment. As shown in Table 4, adsorbate redistribution now occurs within each compartment only and involves the adsorbent in the middle of the adsorber. The effects can be seen on the changes in $\tilde{T}$ for some remarkable points: A, G and the discontinuities appearing in the middle of the branches FG and HA (points W, X, Y and Z). These changes are analysed further on for the cooling half-cycle. Tables 3 and 4 show that implementing two vapour compartments replaces a noticeable transport of adsorbate directly from the hot end (point F) to the cold end (point G) of the

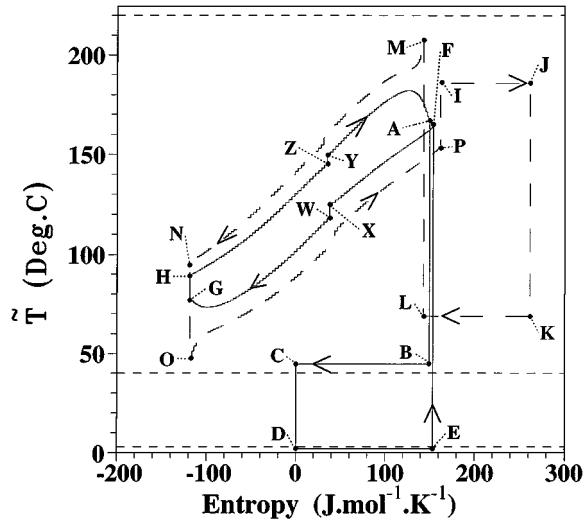

Figure 9. Representation of cycle 2 in the $\tilde{T} - \Delta S$ entropic diagram. The discontinuities on the branches FG, HA, MN and OP show the presence of two compartments in the adsorber.

adsorber by two smaller transports of adsorbate: one from the hot end to the middle of the adsorber (point X) and one from the middle of the adsorber (point W) to the cold end of the adsorber. The effects on the $\tilde{T} - \Delta S$ adsorption cycle can be seen by comparing Figs. 6 and 9. From Figs. 6 to 9, $\tilde{T}$ is increased for points X and F, and symmetrically $\tilde{T}$ is decreased for points W and G. These modifications of $\tilde{T}$ due to modifications in the process of internal adsorbate redistribution would be too long to explain in detail here. Let us just mention that when adsorption of vapour during the cooling period occurs somewhere earlier than it would without vapour redistribution (e.g., for point G), the adsorption heat is then also released at a higher temperature. As a consequence, the corresponding entropic mean temperature $\tilde{T}$ is increased. Reducing the adsorbate redistribution then lowers the $\tilde{T}$ of point G, which gives an explanation for the paradox mentioned above.

Indeed, calculations can be performed with absolutely no vapour redistribution, i.e., with as many 'vapour compartments' as the number of discrete elements in the model. Again, none of the entropy changes is modified, but point A becomes the maximum of the curve HA and point G the minimum of the curve FG.

Why is Performance Unchanged?

This section attempts to develop physical answers to this question with the help of first and second laws analyses.

First Law Analysis

First law analysis explains our results when the whole adsorber and the whole half-cycle are considered.

First, a whole half-cycle consists of a subperiod in isosteric condition and a subperiod under a constant vapour pressure. When a volume of adsorbent undergoes a temperature decrease in isosteric condition, it releases only sensible heat ($\partial\varepsilon/\partial t = 0$, in Eq. (A3)). When this volume undergoes a temperature decrease under a constant vapour pressure, now latent heat of adsorption is involved and the heat released for a same temperature decay is increased: the 'apparent heat capacity' of the adsorbent has significantly increased. It results that the adsorbent is more rapidly cooled in the former configuration than in the latter one. This point, and not the internal adsorbate redistribution, is the basic reason for the sudden change of slope on the breakthrough curve in Fig. 4(a), when the adsorption begins.

Second, when it occurs, the internal adsorbate redistribution is a mass transfer from the hot side of the adsorber to its cold side. Adsorption is exothermic, consequently the adsorbent in the hot side of the adsorber takes some heat from the HTF in order to desorb some vapour. This vapour is re-adsorbed in the cold side of the adsorber and sorption heat is released toward the HTF. As the mass desorbed equals the re-adsorbed mass, the former energy required for desorption is very close to the later energy released by adsorption. For the HTF, the global heat balance is scarcely modified by the adsorbate redistribution. Therefore, the globally averaged fluid temperature at the outlet of the adsorber is the almost the same with or without the adsorbate redistribution. This explains why the energy required from the heating system is not modified.

Second Law Analysis

In the internal adsorbate redistribution, some vapour is desorbed from the hot side of the adsorber and is adsorbed in its cold side. However, the sorption phase change between adsorbed phase and vapour fundamentally does not produce any entropy: the heat released by adsorption (or required for desorption) is directly exchanged with the adsorbent itself, i.e., without any temperature step. Indeed, oppositely to other solid-gas reactions such as chemical (e.g., chlorides + ammonia) or hydriding reaction, adsorption is thermodynamically reversible: a tiny change in the conditions is sufficient for reversing the process. In other words, the adsorption or desorption process by itself does not induce any entropy production. The local heat exchanges between the adsorbent and HTF are modified: the heat flux density, the resulting temperature difference and therefore the entropy production are increased in one part of the adsorber, but they are also reduced in the other part of the adsorber. It finally results that the internal adsorbate redistribution does not generate any entropy due to adsorption or desorption heat[1] and therefore does not affect the cycle performance. This zero entropy production can also be seen in the $\tilde{T} - \Delta S$ diagram: there are only changes in local values of $\tilde{T}$ inside the adsorber (i.e., on the branches FG, HA, MN and OP), but there is absolutely no change in the entropy values.

Adsorber with More than Two Vapour Compartments

These two analyses, with the help of the first and second laws, make it clear that conclusions of the present study are valid for any system using a reversible adsorption pair. In addition, the periodical operation of an adsorber with three and five compartments have been calculated, still with the same operating conditions as for cycle 1. Performance are reported in Table 1, respectively cycle 3 and cycle 5. It can be seen that for any number of vapour compartments, performance are very close to those of cycle 1. Indeed, the temperature profiles are again the same as those presented in Fig. 2 within less than 1 K. The corresponding breakthrough curves are shown in Fig. 10, except for cycle 3 for the sake of clarity. It can be seen that, as described

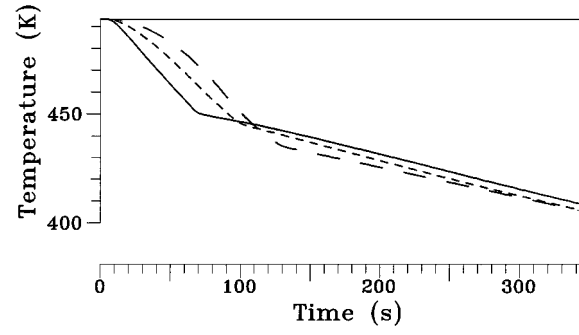

Figure 10. Breakthrough curves during the cold period of (i) cycle 1 (1 compartment, solid lines); (ii) cycle 2 (2 compartments, short dashes); (iii) cycle 5 (5 compartments, long dashes). Increasing the number of compartments does not change the area lying above the breakthrough curve.

above, the breakthrough curves cross each other. As a consequence, the surface lying above each curve is always the same. The present analysis is valid for any number of vapour compartments, which is completely consistent with the physical explanation given in the two previous paragraphs.

Conclusions

The internal adsorbate redistribution occurring in adsorbers during pressurisation or depressurisation under globally isosteric conditions is a phenomenon which is specific to adsorption systems, mainly because the solid-gas equilibrium is divariant. Analysis shows that this phenomenon does not affect the performance of adsorption cycles with heat regeneration. The thermodynamic reasons are completely developed, thanks to the second law analysis and the $\tilde{T} - \Delta S$ diagram that are very useful and powerful tools. Very general conclusions, physically based, can then be drawn from the study of one particular case.

The present study also has a very practical conclusion: in an adsorptive refrigeration unit operated with heat regeneration, there is no need for installing several vapour compartments in the adsorber, each of them being equipped with one check valve for condensation and a second one for evaporation. Indeed, an unit with only one vapour compartment and only two check valves per adsorber will have exactly the same performance.

Appendix: Description of the Model

Heat Transfer Equations and Adsorption State Equation

After the assumptions described in the paragraph '*Modelling*', the equations of the model for the HTF, the metal tube and the adsorbent are respectively,

$$\rho_f \cdot A_f \cdot C_{pf} \cdot \frac{\partial T_f}{\partial t} + \dot{m}_f \cdot C_{pf} \cdot \frac{\partial T_f}{\partial z} = -h_f \cdot \Pi_f \cdot (T_f - T_m) + \lambda_f \cdot A_f \cdot \frac{\partial^2 T_f}{\partial z^2} \quad \text{(A1)}$$

$$\rho_m \cdot A_m \cdot C_{pm} \cdot \frac{\partial T_m}{\partial t} = h_f \cdot \Pi_f \cdot (T_f - T_m) - h'_s \cdot \Pi_s \cdot (T_m - T_s) \quad \text{(A2)}$$

$$\rho_s \cdot A_s \cdot (C_{ps} + \varepsilon \cdot C_{pa}) \cdot \frac{\partial T_s}{\partial t} + \rho_s \cdot A_s \cdot \Delta H' \cdot \frac{\partial \varepsilon}{\partial t} = h'_s \cdot \Pi_s \cdot (T_m - T_s) \quad \text{(A3)}$$

The fluid inlet temperature is constant and all the other boundaries are adiabatic. This model is widely described by Sun et al. (1997), especially with respect to heat transfer. In the present article, attention is focused on the adsorption heat source term: $(\Delta H' \cdot \partial\varepsilon/\partial t)$, which is exactly resolved. First, when required, the model takes into account the sensible heat of the vapour coming from the evaporator and being superheated by the adsorbent before being adsorbed. Therefore, the heat of adsorption just is simply modified according to:

$$\Delta H' = \Delta H + \delta \cdot C_{pg} \cdot (T_s - T_e) \quad \text{(A4)}$$

where δ equals one during the adsorption-evaporation subperiod and zero during the rest of the cycle. The adsorbed flow rate $\partial\varepsilon/\partial t$ is decomposed according to

$$\frac{\partial \varepsilon}{\partial t} = \left(\frac{\partial \varepsilon}{\partial T}\right)_P \cdot \frac{\partial T_s}{\partial t} + \left(\frac{\partial \varepsilon}{\partial P}\right)_T \cdot \frac{\partial P}{\partial t} \quad \text{(A5)}$$

The two partial derivatives of the adsorbed mass ($\partial\varepsilon/\partial T$ and $\partial\varepsilon/\partial P$) and the isosteric heat of adsorption ΔH are obtained from the state equation of the adsorption pair. The state equation used in the model is the one established by Dubinin:

$$\varepsilon_{(T,P)} = W_0 \cdot \rho_L \cdot \exp\left\{-\left[\frac{R \cdot T \cdot \ln\left(P_{s(T)}/P\right)}{E}\right]^2\right\} \quad \text{(A6)}$$

where W_0 is the maximal adsorbable volume in the micropores of the adsorbent, ρ_L is the specific mass of the adsorbed phase assumed to be that of the saturated liquid at the same temperature T, P_s is the saturation pressure at the temperature T and E is an energy characteristic of the adsorption pair. In the case of zeolite NaX + Water, $W_0 = 0.31 \times 10^{-3}\,\mathrm{m^3 \cdot kg^{-1}}$ and $E = 19.6\,\mathrm{kJ \cdot\ mol^{-1}}$. The Dubinin equation is valid over a wide range of concentrations, but it is inconsistent in the Henry's law domain and in the domain close to saturation. From our experience, it is well adapted for calculating refrigeration cycles, because these cycles deal with large variations of concentration while not interfering with those two problematic domains.

The first term on the right-hand side of Eq. (A5) can be numerically treated as a highly nonlinear accumulation term, similar to the first term on the left-hand side of Eq. (A3). The second term on the right-hand side of Eq. (A5) is numerically treated as an explicit source term. First, during each globally isosteric subperiod, the variation of pressure, which is uniform in the adsorber, is ruled by the condition of a constant total adsorbed mass:

$$\int_0^L A_s \cdot \rho_s \cdot \varepsilon_{(T_s(z,t),P(t))} \cdot dz = \int_0^L A_s \cdot \rho_s \cdot \varepsilon_{(T_s(z,0),P(0))} \cdot dz = \text{const.} \quad \text{(A7)}$$

Second, during the desorption (or adsorption) subperiod, pressure is constant and it ideally equals the saturation pressure at the condenser (or evaporator) temperature. As a consequence, this second part of the source term vanishes.

In the case of an adsorber with several vapour compartments, the pressure in each compartment is calculated with the help of equations similar to Eq. (A7), but with integration limits corresponding to the compartment boundaries. Of course, when the considered compartment opens, then the vapour pressure in this compartment becomes constant as explained above.

In addition, as the Dubinin equation is explicit in ε and in P, the isosteric heat of adsorption can easily be deduced from it, according to

$$\Delta H = R \cdot \left(\frac{\partial \ln P}{\partial 1/T} \right)_{\varepsilon} \quad \text{(A8)}$$

Heat Balance and Entropic Mean Temperature

In the following, are presented the equations used in the model for calculating ΔS and $\tilde{T}$ of an elementary length in the adsorber, Δz. After integration over the whole half-cycle, the total heat received by this volume is

$$\Delta Q = \Delta z \cdot \rho_f \cdot A_f \cdot \int_0^{tc/2} C_{pf} \cdot dT_f + \Delta z \cdot \rho_m \cdot A_m \cdot \int_0^{tc/2} C_{pm} \cdot dT_m + \Delta z \cdot \rho_s \cdot A_s \cdot \left[\int_0^{tc/2} (C_{ps} + \varepsilon \cdot C_{pa}) \cdot dT_s + \int_0^{tc/2} \Delta H' \cdot d\varepsilon \right] \quad \text{(A9)}$$

where $\Delta H'$ is defined according to Eq. (A4). Considering Eq. (A5), Eq. (A9) can be rearranged as

$$\Delta Q = \Delta z \cdot \rho_f \cdot A_f \cdot \int_0^{tc/2} C_{pf} \cdot dT_f + \Delta z \cdot \rho_m \cdot A_m \cdot \int_0^{tc/2} C_{pm} \cdot dT_m + \Delta z \cdot \rho_s \cdot A_s \cdot \left[\int_0^{tc/2} \left(C_{ps} + \varepsilon \cdot C_{pa} + \Delta H' \cdot \left(\frac{\partial \varepsilon}{\partial T} \right)_P \right) \cdot dT_s + \int_0^{tc/2} \Delta H' \cdot \left(\frac{\partial \varepsilon}{\partial P} \right)_T \cdot dP \right] \quad \text{(A10)}$$

The corresponding entropy change can be easily deduced from the latter equation:

$$\Delta S = \Delta z \cdot \rho_f \cdot A_f \cdot \int_0^{tc/2} C_{pf} \cdot d\ln T_f + \Delta z \cdot \rho_m \cdot A_m \cdot \int_0^{tc/2} C_{pm} \cdot d\ln T_m + \Delta z \cdot \rho_s \cdot A_s \cdot \left[\int_0^{tc/2} \left(C_{ps} + \varepsilon \cdot C_{pa} + \Delta H' \cdot \left(\frac{\partial \varepsilon}{\partial T} \right)_P \right) \cdot d\ln T_s + \int_0^{tc/2} \frac{\Delta H'}{T} \cdot \left(\frac{\partial \varepsilon}{\partial P} \right)_T \cdot dP \right] \quad \text{(A11)}$$

The entropic mean temperature $\tilde{T}$ is defined as follows. Let us consider a reference volume with uniform temperature that receives a heat power, $\dot{Q}_{(t)}$, during the time interval $[t_0, t_1]$. This volume receives the amount of energy ΔQ. This energy ΔQ makes its temperature $T_{(t)}$, change from T_0 to T_1, and its entropy change by ΔS. Then, as described by Neveu and Castaing-Lasvignottes (1996) and Meunier et al. (1997), an entropic mean temperature $\tilde{T}$ can be defined as the temperature at which the heat quantity ΔQ induces the entropy change ΔS. $\tilde{T}$ usually lies between T_0 and T_1.

$$\tilde{T} = \frac{\Delta Q}{\Delta S} = \frac{\int_{t_0}^{t_1} \dot{Q}_{(t)} \cdot dt}{\int_{t_0}^{t_1} \frac{\dot{Q}_{(t)}}{T_{(t)}} \cdot dt} \quad \text{(A12)}$$

In the present case, ΔQ and ΔS appearing in Eq. (A12) are given by the Eqs. (A10) and (A11).

Nomenclature

A_i	Cross-section in the adsorber	m^2
COP	Cooling Coefficient of Performance	—
C_{pi}	Specific heat	$J \cdot kg^{-1} \cdot K^{-1}$
h_i, h'_i	Heat transfer coefficient	$W \cdot m^{-2} \cdot K^{-1}$
L	Length of the adsorber	m
L_{ev}	Latent heat of evaporation	$J \cdot kg^{-1}$
$\dot{m}_f$	HTF mass flow rate	$kg \cdot s^{-1}$
P	Pressure	Pa
P_s	Saturation pressure	Pa
Q_i	Heat quantity	J
$\dot{Q}_i$	Exchanged power rate	W
R	Ideal gas constant	$J \cdot kg^{-1} \cdot K^{-1}$
t	Time	s
T_i	Temperature	K
$\tilde{T}$	Entropic mean temperature	K
$T_f^{o,c}$	Outlet fluid temperature during the cooling period	K
z	Axial position in the adsorber	m

Greek Letters

ε	Adsorbate concentration	$kg \cdot kg^{-1}$
ΔH	Isosteric heat of adsorption	$J \cdot kg^{-1}$
Δm	Amount of refrigerant cycled during a half-cycle	kg
ΔQ	Enthalpy change due to heat transfer	J
ΔS	Entropy change due to heat transfer	$J \cdot K^{-1}$
λ_i	Thermal conductivity	$W \cdot m^{-1} \cdot K^{-1}$
Π_i	Interface perimeter in the adsorber	m
ρ_i	Specific mass	$kg \cdot m^{-3}$

Subscript

a	Adsorbed phase
c	condenser
e	evaporator
f	fluid
g	refrigerant in gas phase
L	refrigerant in liquid phase
m	metal
s	adsorbent
CS	cooling system
HS	heating system

Acknowledgments

This work was supported by the European Community Joule Contract No JOU2-CT94-0445.

Note

1. As a matter of fact, adsorbate redistribution induces a small entropy production. This irreversibility is due to the temperature difference between the adsorbent that desorbs the vapour (hot side of the adsorber) and the one that adsorbs it (cold side). This irreversibility is then proportional to the sensible heat released by the vapour during this transport from the hot to cold side of the adsorber. It is very small and explains the tiny differences between cycle 1 and cycle 5 in Table 1. This irreversibility due to sensible heat has nothing in common with the phenomena described in Table 2, where latent heat of adsorption (or desorption) is involved.

References

Collier, R.K. and B.M. Cohen, "An Analytic Examination of Methods for Improving the Performance of Desiccant Cooling Systems," *ASME Trans., J. Solar Energy Engng.*, **113**, 157–163 (1991).

Critoph, R.E., "Gas-Fired Air Conditioning Using a Carbon-Ammonia Convective Thermal Wave Cycle," *Proc. Int. Absorption Heat Pump Conference*, Montreal, pp. 353–360, 1996a.

Critoph, R.E., "Performance Estimation of Convective Thermal Wave Adsorption Cycles," *Applied Thermal Engng.*, **16**(5), 429–437 (1996b).

Fueller, T.A., W.J. Wepfer, S.V. Shelton, and M.W. Ellis, "A Two-Temperature Model of the Regenerative Solid-Vapor Heat Pump," *J. Energy Res. Tech. ASME Trans.*, **116**, 297–304 (1994).

Grenier, Ph., J.J. Guilleminot, F. Meunier, and M. Pons, "Solar Powered Solid Adsorption Cold Store," *A.S.M.E. Trans.-J. Solar Energy Eng.*, **110**, 192–197 (1988).

Guilleminot, J.J., F. Meunier, and J. Pakleza, "Heat and Mass Transfer in a Nonisothermal Fixed Bed Solid Adsorbent Reactor: A Uniform Pressure, Nonuniform Temperature Case," *Int. J. Heat Mass Transfer*, **30**(8), 1595–1606 (1987).

Hajji, A. and W.M. Worek, "Simulation of a Regenerative, Closed-Cycle Adsorption Cooling/Heating System," *Energy*, **16**(3), 643–654 (1991).

Härkönen, M. and A. Aittomaki, "The Principle of Internal Regeneration as Applied to the Adsorption Heat Pump Process," *Heat Recovery Systems and CHP*, **11**(4), 239–248 (1991).

Istria, S., J. Castaing-Lasvignottes, and P. Neveu, "Energetic Analysis, Application Field and Performance of a New Thermochemical Sorption Cycle: The Multisalt System," *Applied Thermal Engng.*, **16**(11), 875–889 (1996).

Istria, S., C. Roque, J. Castaing-Lasvignottes, V. Goetz, and P. Neveu, "Nouveaux Procédés de Transformateur Thermochimique Incluant la Mise en Oeuvre de Réacteurs Multisels et Utilisant des Fronts de Chaleur," *Proc. 19th Int. Congress Refrigeration*, IIF/IIR, Vol. IIIa, pp. 107–114, 1995.

Jones, J.A., "Carbon/Ammonia Regenerative Adsorption Heat Pump," *Proc. Int. Absorption Heat Pump Conf., ASME*, Vol. AES-31, pp. 449–455, 1993.

Kuma, T., T. Hirose, M. Goto, and A. Kodama, "Thermally Activated Honeycomb Dehumidifier for Adsorption Cooling System," *ASME Trans., Solar Engineering*, **2**, 1267–1275 (1995).

Ludwig, J., "Adsorptionswärmepumpe mit 2 Adsorbern," *Brennstoff-Wärme-Kraft*, **47**(3), 94–96 (1995).

Meunier, F., "Solid Sorption: An Alternative to CFCs," *Heat Recovery Systems and CHP*, **13**(4), 289–296 (1993).

Meunier, F., P. Neveu, and J. Castaing-Lasvignottes, "Comparison of Sorption Systems Based on Equivalent Carnot Cycles," accepted for presentation in *ASHRAE Winter meeting*, Philadelphia, Jan. 25–29, 1997.

Miles, D.J., D.M. Sanborn, G. Nowakowski, and S.V. Shelton, "Gas Fired Sorption Heat Pump Development," *Heat Recovery Systems and CHP*, **13**(4), 347–351 (1993).

Miles, D.J. and S.V. Shelton, "Coupled Heat Transfer and Thermodynamic Adsorption Heat Pump Analysis," *Heat Pump Design, Analysis and Application, A.S.M.E.*, Vol. AES-26, pp. 33–38, 1991.

Miles, D.J. and S.V. Shelton, "Design and Testing of a Solid-Sorption Heat Pump System," *Applied Thermal Eng.*, **16**(4), 389–394 (1996).

Miller, E.B., "The Development of Silica Gel Refrigeration," *The American Society of Refrigeration Engineers*, **17**(4) (1929).

Neveu, P. and J. Castaing-Lasvignottes, "Analyse Thermodynamique des Transformateurs Thermochimiques Solide/Gaz," *Proc. Int. Ab-sorption Heat Pump Conference*, Montreal, pp. 261–268, 1996.

Pons, M., "Second Law Analysis of Adsorption Cycles with Thermal Regeneration," *J. Energy Res. Tech., ASME Trans.*, **118**, 229–236 (1996).

Pons, M., "Analysis of the Adsorption Cycles with Thermal Regeneration Based on the Entropic Mean Temperatures," *Applied Thermal Eng.*, **17**(7), 615–627 (1997).

Pons, M., D. Laurent, and F. Meunier, "Experimental Temperature Fronts for Adsorptive Heat Pump Applications," *Applied Thermal Eng.*, **16**(5), 395–404 (1996).

Pons, M. and S. Szarzynski, "Optimized Internal Vapour Transports for Adsorption Cycles with Thermal Regeneration," *Proc. Int. Ab-sorption Heat Pump Conference*, Montreal, pp. 421–428 (1996).

Shelton, S.V., W.J. Wepfer, and D.J. Miles, "Ramp Wave Analysis of the Solid Vapor Heat Pump," *J. Energy Res. Tech. ASME Trans.*, **112**, 69–78 (1990).

Sun, L.M., N. Ben Amar, and F. Meunier, "Numerical Study on Coupled Heat and Mass Transfers in an Adsorber with External Fluid Heating," *Heat Recovery Systems and CHP*, **15**(1), 19–29 (1995).

Sun, L.M., Y. Feng, and M. Pons, "Numerical Investigation of Adsorptive Heat Pump Systems with Thermal Wave Heat Regeneration under Uniform-Pressure Conditions," *Int. J. Heat Mass Transfer*, **40**(2), 281–293 (1997).

Szarzynski, S., Y. Feng, and M. Pons, "Study of Different Internal Vapour Transports for Adsorption Cycles with Thermal Regeneration," *Int. J. Refridgeration*, **20**(6), 390–401 (1997).

Willers, E., M. Groll, A. Isselhorst, and W. de Jong, "Advanced Concept of a Metal Hydride Solid Sorption Device for Combined Heating and Airconditioning," *Proc. Int. Ab-sorption Heat Pump Conf.*, Montreal, pp. 169–175, 1996.

Zheng, W. and W.M. Worek, "Readsorption Processes in a Sorption Bed Heat Exchanger During Pressurization and Depressurization," *J. Heat Transfer ASME Trans.*, **117**, 865–870 (1995).

Zheng, W., W.M. Worek, and G. Nowakowski, "Effect of Design and Operating Parameters on the Performance of Two-Bed Sorption Heat Pump Systems," *J. Energy Res. Tech. ASME Trans.*, **117**, 67–74 (1995a).

Zheng, W., W.M. Worek, and G. Nowakowski, "Performance Optimization of Two-Bed Closed-Cycle Solid-Sorption Heat Pump Systems," *Heat Mass Transfer*, **31**, 1–9 (1995b).